AIAA JOURNAL
Vol. 30, No. 3, March 1992

Discretization Errors Inherent in Finite Difference Solution of Propeller Noise Problems

Christopher K. W. Tam*
Florida State University, Tallahassee, Florida 32306

Global errors arising from the use of a finite difference approximation to solve propeller noise problems are investigated. It is found that the calculated waveforms of the finite difference solutions are subjected to severe distortion due to dispersive effects. This is so even when the Fourier amplitudes of the different blade-passage harmonics of the acoustic disturbance of the propeller are adequately predicted. In addition, it is found that finite difference solutions can produce spurious acoustic radiation. The spurious radiation is a form of aliasing error. The relative intensity of the spurious acoustic radiation can become significant at high subsonic flight Mach number and at high subsonic blade-tip rotational Mach number. Also, the relative intensity is higher for the higher order blade-passage harmonics.

I. Introduction

THIS paper deals with the computation of noise generated by high-speed propellers. To predict propeller noise, the present day practice is to calculate first the loading on the blades. This is usually done by a computational fluid dynamics (CFD) code. Once the loading is determined, a hybrid analytical and computational acoustic code is used to determine the noise radiated.[1-6] This two-step method is usually a compromise. The CFD code that is based on the fully nonlinear equations of motion and the acoustic code that assumes that the solution is linear are not always compatible and consistent. A true computational solution of the propeller noise problem is one that solves the aerodynamics and noise problems simultaneously. Such a computational aeroacoustics method is not available at the present time. The objective of the present paper is to examine global errors that the computational aeroacoustics approach must overcome if a finite difference approximation is used. By better understanding the nature of the errors and by being able to make estimates of their magnitudes, it is hoped that such errors can either be minimized, avoided, or suppressed in some way.

A popular way to calculate the loading and noise from propellers is to approximate the governing equations (Euler equations) by a set of finite difference equations. By replacing the partial differential equations by finite difference equations, some inherent errors are inadvertently created. A familiar type of error is the so-called truncation error (related to the order of terms dropped in approximating derivatives by finite differences). Truncation error of this type is local in nature. It degrades the accuracy of the solution but is usually tolerable. However, there are other types of errors that are more subtle and are global (cumulative) in nature. For acoustic wave propagation problems, the characteristics of the medium described by the partial differential equation are not the same as those described by the finite difference equation. Among the errors of this category are the effects of dispersion and damping. Damping, sometimes introduced artificially in a numerical scheme to assure computational stability, causes the wave amplitude to decrease. The characteristics of the solution are, however, usually preserved. An acoustic medium governed by the Euler equations is nondispersive. The speed of propagation is the same for all frequencies. A medium governed by the finite difference equations that approximate the Euler equations is dispersive.[7-8] The dispersion effect, which causes different frequency components to propagate with different speeds, does not affect the amplitude of each frequency component of the solution as in the case of damping. But by shifting the components in time and space relative to each other, the nature of the total solution is generally greatly affected or destroyed, especially after propagating over a fairly long distance. For propeller noise problems the dispersion effect is usually a more damaging form of error. It can provide totally misleading results.

In this paper the effect of dispersion due to a finite difference approximation on the computed propeller noise solution is examined. The controlling parameters of the phenomenon are the rotational frequency, the flight Mach number, the number of blades, the mesh size, and the distance of propagation. The latter is important because the dispersive effect is cumulative. For the purpose of examining the nature and consequences of dispersive effects on the propagation of propeller noise, the linear acoustics problem is considered. The linear model is generally applicable away from the surfaces of the blades over the intervening region between the propeller and the distant observer. It is in this region of wave propagation, where the use of linearized equations is justified, that the cumulative dispersive effect is important.

In this study a blade-fixed coordinate system following the work of Ref. 6 will be employed. The reason for using the blade-fixed coordinate system is that in this frame of reference the acoustic wave field is time independent. The governing equation is discretized and the finite difference equation is solved. The solution is constructed by the methods of discrete and continuous Fourier transforms. This method of solving the governing finite difference equation, although not widely used, avoids any numerical round-off errors and numerical acoustic reflections arising from the necessity of imposing a radiation boundary condition at the edge of the finite computational domain. Such errors and complications are inevitable in any direct numerical solution. It is to be noted that if handled incorrectly these later types of errors may overwhelm or, at least, so contaminate the calculated solution that a clear and straightforward way of evaluating the dispersive effect becomes difficult if not impossible. Numerical results of the solutions indicate that because of dispersion the waveform of the acoustic disturbances of a high-speed propeller cannot be accurately predicted by a finite difference approximation unless a large number of grid points are used. The magnitudes of the first few Fourier harmonics, however, can be fairly accurately computed by finite difference schemes with reasonable mesh

Received Sept. 20, 1990; presented as Paper 90-3943 at the AIAA 13th Aeroacoustics Conference, Tallahassee, Florida, Oct. 22-24, 1990; revision received April 6, 1991; accepted for publication April 16, 1991.

*Professor, Department of Mathematics. Associate Fellow AIAA.

size. One implication of these findings is that to obtain an accurate prediction of the waveform of propeller noise the development of finite difference schemes with minimum dispersion is desirable and needed.

II. Formulation of the Propeller Noise Problem

Consider a high-speed propeller moving with forward velocity u_∞ and angular velocity ω as shown in Fig. 1. In a coordinate system fixed to the center of the propeller, the linearized equations of motion of an inviscid, compressible fluid are

$$\frac{\partial \rho}{\partial t} + u_\infty \frac{\partial \rho}{\partial x} + \rho_\infty \nabla \cdot \mathbf{v} = 0 \tag{1}$$

$$\rho_\infty \left(\frac{\partial \mathbf{v}}{\partial t} + u_\infty \frac{\partial \mathbf{v}}{\partial z} \right) = -\nabla p \tag{2}$$

$$p = a_\infty^2 \rho \tag{3}$$

Here ρ, $\mathbf{v}$, and p are the perturbation density, velocity, and pressure, respectively; ρ_∞ and a_∞ are the ambient density and the speed of sound of the fluid. Since the flow is irrotational, it is convenient to introduce a velocity potential Φ such that

$$\mathbf{v} = -\nabla \Phi \tag{4}$$

By Eq. (2) the velocity potential is related to the pressure perturbation by

$$p = \rho_\infty \left(\frac{\partial \Phi}{\partial t} + u_\infty \frac{\partial \Phi}{\partial z} \right) \tag{5}$$

Upon eliminating the other variables, it is straightforward to find that Φ satisfies the convective wave equation:

$$\nabla^2 \Phi - \frac{1}{a_\infty^2} \left(\frac{\partial}{\partial t} + u_\infty \frac{\partial}{\partial z} \right)^2 \Phi = 0 \tag{6}$$

In the blade-fixed rotating frame of reference, the propeller noise problem is time independent. Let (r,θ_s,z) be the cylindrical coordinates of the stationary coordinate system and (r,θ,z) be those of the blade-fixed coordinate system; then

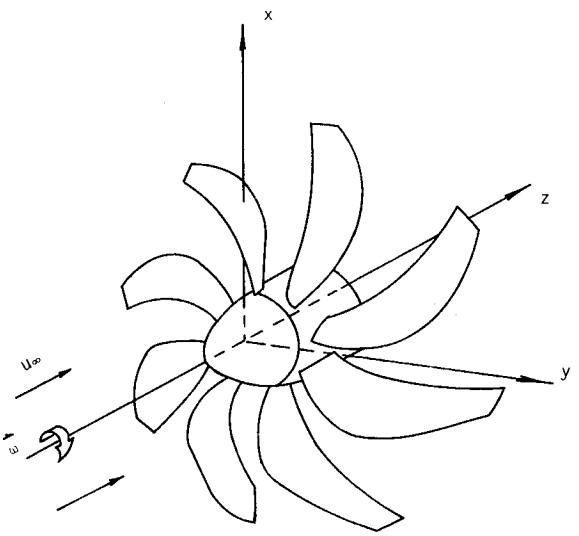

Fig. 1 High-speed propeller with forward velocity u_∞ and angular velocity ω as seen in the coordinate system fixed to the center of the propeller.

$$\theta = \theta_s - \omega t, \qquad \frac{\partial}{\partial t} \to -\omega \frac{\partial}{\partial \theta}, \qquad \frac{\partial}{\partial \theta_s} \to \frac{\partial}{\partial \theta} \tag{7}$$

In the blade-fixed coordinate system, Eq. (6) becomes

$$\left(\frac{\partial^2}{\partial r^2} + \frac{1}{r}\frac{\partial}{\partial r} + \frac{1}{r^2}\frac{\partial^2}{\partial \theta^2} + \frac{\partial^2}{\partial z^2} \right) \Phi - \frac{1}{a_\infty^2} \left(u_\infty \frac{\partial}{\partial z} - \omega \frac{\partial}{\partial \theta} \right)^2 \Phi = 0 \tag{8}$$

The noise of a high-speed propeller is generated by the thickness of the blade and the loading on the blade. These are referred to as the thickness and loading noise.[1-6] As has been discussed in some detail in Ref. 6, the thickness and loading on the blade can be modeled by adding appropriate nonhomogeneous terms on the right-hand side of Eq. (8). The general thickness and loading noise problems are, therefore, governed by an inhomogeneous equation of the form

$$\frac{\partial^2 \Phi}{\partial r^2} + \frac{1}{r}\frac{\partial \Phi}{\partial r} + \frac{1}{r^2}\frac{\partial^2 \Phi}{\partial \theta^2} + \frac{\partial^2 \Phi}{\partial z^2} - \frac{1}{a_\infty^2} \left(u_\infty \frac{\partial}{\partial z} - \omega \frac{\partial}{\partial \theta} \right)^2 \Phi = f(r,\theta,z) \tag{9}$$

For the purpose of investigating the dispersion effect on the finite difference solutions of propeller noise problems, it is sufficient to study the fundamental solution of Eq. (9) obtained by replacing the right-hand side by a δ function on each blade. That is,

$$\nabla^2 \Phi - \frac{1}{a_\infty^2} \left(u_\infty \frac{\partial}{\partial z} - \omega \frac{\partial}{\partial \theta} \right)^2 \Phi = \sum_{j=0}^{B-1} Q \delta \left(\theta - \frac{2\pi j}{B} \right) \frac{\delta(r - L)}{r} \delta(z) \tag{10}$$

In Eq. (10) Q is the source strength, B is the number of blades, and L (the radial distance of the source from the rotational axis) will be taken to be the blade length as most of the noise is generated at the tip regions of the blades.

The z and θ dependence of Eq. (10) will now be discretized in increments of Δz and $\Delta \theta$, respectively. This means that the velocity potential Φ will be replaced by

$$\Phi(r,\theta,z) \to \Phi(r,n\Delta\theta,m\Delta z) \equiv \Phi_n^m(r) \tag{11}$$

where n and m are integers. Since there are B blades, $\Delta\theta$ will be taken to be equal to

$$\Delta\theta = 2\pi/(NB) \tag{12}$$

where N is the number of points per blade. For convenience, N is taken to an even integer. A second-order accurate central difference approximation for the first and second derivatives in θ and z will be used. The r dependence in Eq. (10) will, however, not be discretized so that the overall finite difference scheme is in the form of the well-known method of lines. In conjunction with the discretization in z and θ the delta functions $\delta(z)$ and $\delta(\theta - 2\pi j/B)$ are approximated by discrete step functions extending over a distance Δz and $\Delta\theta$ with corresponding heights such that the areas of the functions are unity. If $H(z)$ denotes the unit step function and $\delta_{i,j}$ is the Kronecker delta, then these delta functions are replaced by

$$\delta(z) = [H(z + \Delta z/2) - H(z - \Delta z/2)]/\Delta z \tag{13a}$$

$$\delta(\theta - 2\pi j/B) = \delta_{n,jN}/(\Delta\theta), \qquad j = 0, 1, 2, \ldots, B - 1 \tag{13b}$$

Upon incorporating all of the above discrete approximations, Eq. (10) becomes

$$\frac{d^2\Phi_n^m}{dr^2} + \frac{1}{r}\frac{d\Phi_n^m}{dr} + \frac{\Phi_{n+1}^m - 2\Phi_n^m + \Phi_{n-1}^m}{r^2(\Delta\theta)^2} + \frac{\Phi_n^{m+1} - 2\Phi_n^m + \Phi_n^{m-1}}{(\Delta z)^2} - \frac{1}{a_\infty^2}\left[u_\infty^2\frac{(\Phi_n^{m+1} - 2\Phi_n^m + \Phi_n^{m-1})}{(\Delta z)^2} - u_\infty\omega\frac{(\Phi_{n+1}^{m+1} - \Phi_{n-1}^{m-1} - \Phi_{n+1}^{m+1} + \Phi_{n-1}^{m-1})}{2(\Delta z)(\Delta\theta)} + \omega^2\frac{(\Phi_{n+1}^m - 2\Phi_n^m + \Phi_{n-1}^m)}{(\Delta\theta)^2}\right] = Q\sum_{j=0}^{B-1}\frac{\delta(r-L)}{r(\Delta z)(\Delta\theta)}[H(z+\Delta z/2) - H(z-\Delta z/2)]\delta_{n,jN} \tag{14}$$

where $z = 0$ ($m = 0$) on the right-hand side. Equation (14) is a partial difference differential equation the solution of which will be discussed later.

III. Solution of the Finite Difference Equation

Finite difference equation (14) can be solved numerically in a finite computational domain. But such a solution will inevitably incur numerical round-off errors. In addition, to be able to solve Eq. (14) in this way, a nonreflecting boundary condition must be imposed at the boundary of the finite computational domain. A perfectly transparent radiation boundary condition for pulse-type acoustic disturbances that are typical of the noise of high-speed propellers is currently not available. In other words, some acoustic reflections at the artificial boundary are very likely. For the purpose of studying the dispersion effects on acoustic wave propagation due to finite differencing of the governing equation, these types of computational errors are to be avoided whenever possible. It turns out the finite difference equation (14) can be solved analytically. Such an analytical solution is free from round-off and nontransparent radiation boundary condition errors. It is, therefore, ideal for analyzing the effects of dispersion due to finite difference approximation. The method of solution that follows is new and should be useful for analyzing wave propagation characteristics of linear finite difference equations.

Equation (14) is defined only at a discrete set of points in the z direction, namely, at $z = m\Delta z$, m = integer. Obviously it is a special case of the following more general finite difference differential equation in which z is a continuous variable:

$$\frac{d^2\Phi_n(r,z)}{dr^2} + \frac{1}{r}\frac{d\Phi_n(r,z)}{dr} + \frac{1}{r^2(\Delta\theta)^2}[\Phi_{n+1}(r,z) - 2\Phi_n(r,z) + \Phi_{n-1}(r,z)] + \frac{1}{(\Delta z)^2}[\Phi_n(r,z+\Delta z) - 2\Phi_n(r,z) + \Phi_n(r,z-\Delta z)] - \frac{1}{a_\infty^2}\left\{\frac{u_\infty^2}{(\Delta z)^2}\times[\Phi_n(r,z+\Delta z) - 2\Phi_n(r,z) + \Phi_n(r,z-\Delta z)] - \frac{u_\infty\omega}{2(\Delta z)(\Delta\theta)}[\Phi_{n+1}(r,z+\Delta z) - \Phi_{n+1}(r,z-\Delta z) - \Phi_{n-1}(r,z+\Delta z) + \Phi_{n-1}(r,z-\Delta z)] + \frac{\omega^2}{(\Delta\theta)^2}[\Phi_{n+1}(r,z) - 2\Phi_n(r,z) + \Phi_{n-1}(r,z)]\right\} = Q\sum_{j=0}^{B-1}\frac{\delta(r-L)}{r(\Delta z)(\Delta\theta)}[H(z+\Delta z/2) - H(z-\Delta z/2)]\delta_{n,jN} \tag{15}$$

In Eq. (15) the function $\Phi_n(r,z)$ is defined for all of the values of the independent variable z. Clearly when $z = m\Delta z$ where m = integer, $\Phi_n(r,z)$ is equal to $\Phi_n^m(r)$. Thus the solution of Eq. (14) is contained in the solution of Eq. (15).

Let the discrete Fourier transform in n and the continuous Fourier transform in z and their inverses be defined as follows:

$$\Phi_s(r,z) = \frac{\Delta\theta}{2\pi}\sum_{n=-NB/2}^{NB/2-1}\Phi_n(r,z)\exp(-ins\Delta\theta) \tag{16a}$$

$$\Phi_n(r,z) = \sum_{s=-NB/2}^{NB/2-1}\Phi_s(r,z)\exp(ins\Delta\theta) \tag{16b}$$

where $-NB/2 \le n, s \le NB/2 - 1$;

$$\tilde{\Phi}(r,k) = \frac{1}{2\pi}\int_{-\infty}^{\infty}\Phi(r,z)\exp(-ikz)\,dz \tag{17a}$$

$$\Phi(r,z) = \int_{-\infty}^{\infty}\tilde{\Phi}(r,k)\exp(ikz)\,dk \tag{17b}$$

By means of definitions (16a) and (17a) and the fact that $\Phi_n(r,z)$ is periodic in n with period NB, the transform of $\Phi_{n+1}(r,z + \Delta z)$ can be found in terms of $\tilde{\Phi}_s(r,k)$, the transform of $\Phi_n(r,z)$:

$$\frac{\Delta\theta}{(2\pi)^2}\sum_{n=-NB/2}^{NB/2-1}\int_{-\infty}^{\infty}\Phi_{n+1}(r,z+\Delta z)\exp(-ins\Delta\theta - ikz)\,dz = \tilde{\Phi}_s(r,k)e^{is\Delta\theta + ik\Delta z} \tag{18}$$

Upon applying the discrete Fourier transform to the sum of Kronecker deltas, $\delta_{n,jN}$, on the right-hand side of Eq. (15), it is easy to find

$$\frac{\Delta\theta}{2\pi}\sum_{j=0}^{B-1}\sum_{n=-NB/2}^{NB/2-1}\delta_{n,jN}\exp[-isn(\Delta\theta)] = \frac{1}{NB}\sum_{j=0}^{B-1}\exp(-i2\pi js/B) = \frac{1}{N}\delta_{s,lB}, \quad -N/2 \le \ell \le N/2 - 1 \tag{19}$$

Therefore, by Eq. (19) the discrete Fourier transform of $\Phi_n(r,z)$ is zero unless the discrete transform variable s is equal to ℓB. On accounting for this restriction on the value of s, the Fourier transform (discrete and continuous) of Eq. (15) is easily found to be

$$\frac{d^2\tilde{\Phi}_{\ell B}}{dr^2} + \frac{1}{r}\frac{d\tilde{\Phi}_{\ell B}}{dr} - (\alpha^2 - \beta + \nu^2/r^2)\tilde{\Phi}_{\ell B} = \frac{Q\sin(k\Delta z/2)\delta(r-L)}{\pi(\Delta z)(\Delta\theta)kLN}, \quad -N/2 \le \ell \le N/2 - 1 \tag{20}$$

where

$$\alpha = 2\sin(k\Delta z/2)/\Delta z$$

$$\nu^2 = 4\sin^2(\ell B\Delta\theta/2)/(\Delta\theta)^2$$

$$\beta = \frac{4}{a_\infty^2}\left[\frac{u_\infty^2\sin^2(k\Delta z/2)}{(\Delta z)^2} - \frac{u_\infty\omega}{2(\Delta\theta)(\Delta z)}\sin(k\Delta z)\times\sin(\ell B\Delta\theta) + \frac{\omega^2}{(\Delta\theta)^2}\sin^2(\ell B\Delta\theta/2)\right]$$

The solution of Eq. (20) is

$$\tilde{\Phi}_{\ell B} = \frac{-Q \sin(k\Delta z/2)}{\pi(\Delta z)(\Delta\theta)kN} \begin{cases} I_\nu(\lambda r)K_\nu(\lambda L), & r \le L \\ I_\nu(\lambda L)K_\nu(\lambda r) & r > L \end{cases} \tag{21}$$

where $\lambda = (\alpha^2 - \beta)^{1/2}$ and I_ν and K_ν are the modified Bessel functions of order ν. To satisfy the boundedness and outgoing wave condition far away from the propeller, the following branch of the square root of λ is chosen:

$$-\pi/2 \le \arg(\lambda) \le \pi/2 \tag{22}$$

In Eq. (22) the left-hand equality is used for positive integer ℓ and the right-hand equality is used when ℓ is negative. Now by inverting the discrete and continuous Fourier transforms, the solution of the finite difference differential equation (15) is found:

$$\Phi_n(r,z) \underset{r>L}{=} -\sum_{\ell=-N/2}^{N/2-1} \int_{-\infty}^{\infty} \frac{Q \sin(k\Delta z/2)}{\pi(\Delta z)(\Delta\theta)kN} I_\nu(\lambda L)K_\nu(\lambda r) \times \exp(ikz + inlB\Delta\theta)\, dk \tag{23}$$

To find the radiated sound in the far field, it is more convenient to introduce a spherical coordinate system (R,χ,θ) centered at the origin with the polar axis coinciding with the z axis. The (R,χ,θ) are related to the cylindrical coordinates (r,θ,z) by

$$z = R\cos\chi, \qquad r = R\sin\chi, \qquad \theta = \theta \tag{24}$$

In terms of the spherical coordinates, formula (23) in the far field becomes

$$\Phi_n(R,\chi) \underset{R\to\infty}{\sim} -\sum_{\ell=-N/2}^{N/2-1} \int_{-\infty}^{\infty} \frac{Q \sin(k\Delta z/2)}{\pi(\Delta z)(\Delta\theta)kN} I_\nu(\lambda L) \times \left(\frac{\pi}{2R\sin\chi}\right)^{1/2} \frac{\exp[F(k)R + inlB(\Delta\theta)]}{\lambda^{1/2}}\, dk \tag{25}$$

where $F(k) = -\lambda \sin\chi + ik\cos\chi$. In obtaining Eq. (25), the modified Bessel function K_ν of Eq. (23) has been replaced by its asymptotic formula (large argument). The k integral in the previous formula may now be evaluated asymptotically by the saddle point method. The value of k at the saddle point, i.e., k_s, is given by

$$F'(k_s) = 0, \qquad ' = \frac{d}{dk} \tag{26}$$

It is to be noted that the function $F'(k)$ is periodic in k with period $2\pi/\Delta z$. Therefore, if k_0 is the root of Eq. (26) with the smallest absolute value, then

$$k_j = k_o + 2\pi j/\Delta z, \qquad j = \pm 1, \pm 2, \ldots \tag{27}$$

are also roots of the equation. It is worthwhile to point out at this time that in the exact solution of the original partial differential equation, Eq. (10), there is only one saddle point. The exact saddle point is equal to the value of k_0 in the limit $\Delta z, \Delta\theta \to 0$. For the special case of $\chi = \pi/2$, that is, in the plane of the propeller, Eq. (26) simplifies to

$$(1 - M_\infty^2)\sin(k\Delta z)/\Delta z + M_\infty\omega \sin(\ell B\Delta\theta) \times \cos(k\Delta z)/(a_\infty\Delta\theta) = 0 \tag{28}$$

where $M_\infty = u_\infty/a_\infty$ is the flight Mach number. The root with the smallest absolute value is

$$k_0 = -\frac{1}{\Delta z}\tan^{-1}\left[\frac{M_\infty}{1 - M_\infty^2}\frac{\omega\Delta z \sin(\ell B\Delta\theta)}{a_\infty\Delta\theta}\right] \qquad \ell = \pm 1, \pm 2, \ldots$$

$$k_0 = -\pi/\Delta z, \qquad \ell = 0 \tag{29}$$

Finally, upon evaluating the integral of formula (25) asymptotically,[9] an explicit expression for the discretized velocity potential $\Phi_n(R,\chi)$ in the far field is found:

$$\Phi_n(R,\chi) \underset{R\to\infty}{=} -\sum_{\substack{\ell=-N/2 \\ \ell\neq 0}}^{N/2-1} \frac{Q \sin(k_0\Delta z/2)I_\nu(\lambda_0 L)\exp[F(k_0)R + inlB\Delta\theta - i\pi/4\,\mathrm{sgn}(\ell)]}{N(\Delta z)(\Delta\theta)k_0R(\sin\chi|F''(k_0)|)^{1/2}\lambda_0^{1/2}} \times \left[1 + \sum_{\substack{j=-\infty \\ j\neq 0}}^{\infty} \frac{(-1)^j \exp[i2\pi j(\cos\chi)R/\Delta z]}{1 + 2\pi j/(\Delta z k_0)}\right] \tag{30}$$

where $\lambda_0 = \lambda(k_0)$ and $\mathrm{sgn}(\ell)$ = the sign of ℓ.

IV. Comparison Between the Finite Difference and the Exact Solution

The analytical solution of Eq. (10) for the velocity potential $\Phi(R,\chi,\theta)$ can be constructed according to the procedure described in Ref. 6. A simpler way to find Φ is to set $n\Delta\theta = \theta$ fixed in expression (30) and take the formal limit as $\Delta z \to 0$, $\Delta\theta \to 0$, and $N \to \infty$. On recognizing that the terms with negative integer ℓ are the complex conjugates of the corresponding terms with positive ℓ, it is straightforward to find, after substitution into Eq. (5), that the pressure field generated by the propeller is

$$p_n(R,\chi,\theta) \underset{R\to\infty}{=} \frac{-\rho_\infty QB^2\omega}{2\pi R(1 - M_\infty^2\sin^2\chi)^{1/2}} \times \sum_{\ell=1}^{\infty} \ell\left(1 - \frac{u_\infty\cos\chi}{V(\chi)}\right)J_{\ell B}\left(\frac{\omega L}{a_\infty}\frac{\ell B\sin\chi}{(1 - M_\infty^2\sin^2\chi)^{1/2}}\right) \times \sin\left[\ell B\left(\frac{\omega R}{V(\chi)} + \theta - \frac{\pi}{2}\right)\right] \tag{31}$$

where $J_{\ell B}$ is the Bessel function of order ℓB and $V(\chi)$ is the velocity of propagation of the acoustic waves in the radial direction[6]:

$$V(\chi) = u_\infty\cos\chi + (a_\infty^2 - u_\infty^2\sin^2\chi)^{1/2} \tag{32}$$

The pressure waveform of the finite difference solution may be calculated by formula (30) and Eq. (5) using a central difference approximation for the θ derivative. For acoustic radiation in the propeller plane, i.e., $\chi = \pi/2$, great simplification of this formula is possible. On taking into consideration the fact that the terms with positive and negative integer ℓ are complex conjugates of each other and that for large N the $\ell = -N/2$ term may be neglected as being exponentially small, the pressure waveform in the propeller plane is found to be

$$p_n(R,\pi/2) \underset{R\to\infty}{=} -\sum_{\ell=1}^{N/2-1} \frac{\rho_\infty Q\omega B \sin(\ell B\Delta\theta)\sin(k_0\Delta z/2)J_\nu(L\psi)}{\pi\Delta\theta k_0\Delta z|\psi F''(k_0)|^{1/2}} \times \sin\left[\psi R + n\ell B\Delta\theta - \frac{\nu\pi}{2}\right]\left[1 + \sum_{\substack{j=-\infty \\ j\neq 0}}^{\infty} \frac{(-1)^j}{1 + 2\pi j/(k_0\Delta z)}\right] \tag{33}$$

where $\lambda_0 = \psi e^{-i\pi/2}$, $k_0\Delta z$ is given by formula (28):

Table 1 Relative magnitude of spurious radiation, S[a]

ℓ	$N = 20$	$N = 30$	$N = 40$	$N = 100$
1	0.108	0.075	0.025	0.023
2	0.173	0.134	0.108	0.046
3	0.205	0.173	0.146	0.072
4	0.221	0.197	0.173	0.089
5	0.225	0.212	0.192	0.108

[a] $\chi = \pi/2$, $M_\infty = 0.8$, $M_t = 0.8$, $B = 8$, $L/\Delta z = N$

Table 2 Relative magnitude of spurious radiation, S[a]

ℓ	$N = 20$	$N = 30$	$N = 40$	$N = 100$
1	0.017	0.011	0.008	0.001
2	0.032	0.022	0.017	0.001
3	0.044	0.032	0.025	0.002
4	0.052	0.040	0.032	0.002
5	0.054	0.047	0.039	0.003

[a] $\chi = \pi/2$, $M_\infty = 0.3$, $M_t = 0.8$, $B = 8$, $L/\Delta z = N$

$$\nu = (NB/\pi)\sin(\ell\pi/N)$$

$$L\psi = \left[4M_t^2\left(\frac{NB}{2\pi}\right)^2 \sin^2\left(\frac{\ell\pi}{N}\right) - 2M_\infty M_t\left(\frac{L}{\Delta z}\right)\left(\frac{NB}{2\pi}\right)\sin\left(\frac{2\pi\ell}{N}\right)\sin(k_0\Delta z) - 4(1-M_\infty^2)\left(\frac{L}{\Delta z}\right)^2 \sin^2(k_0\Delta z/2)\right]^{1/2}$$

$$|\psi F''(k_0)|^{1/2} = \left\{(1-M_\infty^2)\cos(k_0\Delta z) - M_\infty M_t\left(\frac{\Delta z}{L}\right)\left(\frac{NB}{2\pi}\right)\sin\left(\frac{2\pi\ell}{N}\right)\sin(k_0\Delta z) + \left[(1-M_\infty^2)\left(\frac{L}{\Delta z}\right)\sin(k_0\Delta z) + M_\infty M_t\left(\frac{NB}{2\pi}\right)\sin\left(\frac{2\pi\ell}{N}\right)\cos(k_0\Delta z)\right]^2 \Big/ (L\psi)^2\right\}^{1/2}$$

where $M_t = \omega L/a_\infty$ is the blade-tip rotational Mach number.

By comparing the waveform and other wave characteristics as computed by formula (31) to those calculated by formula (33), it is possible to evaluate the quantitative and qualitative differences between the finite difference and the exact solution. The following major differences are noted.

Spurious Radiation

The terms in the summation over j of the last factor of Eq. (33) have no counterpart in the exact solution of formula (31). These terms represent spurious radiation. The origin of these spurious radiation terms, as pointed out before, is aliasing. This comes about because spatial discretization generally leads to a dispersion function with periodic group velocity in the wave number space. The result is that for a given direction more than one wave number would have matching group velocity for acoustic radiation. The terms involved alternate in sign so that they form an alternating series. As an estimate of the relative magnitude of the spurious radiation to the true acoustic radiation, the magnitude of the first term ($j = 1$) may be used. Thus the relative magnitude of the spurious radiation S is

$$S = \frac{1}{|1 + 2\pi/(k_0\Delta z)|} \tag{34}$$

Table 3 Relative magnitude of spurious radiation, S[a]

ℓ	$N = 20$	$N = 30$	$N = 40$	$N = 50$
1	0.013	0.008	0.006	0.005
2	0.024	0.017	0.013	0.010
3	0.033	0.024	0.018	0.015
4	0.039	0.030	0.024	0.020
5	0.041	0.035	0.029	0.024

[a] $\chi = \pi/2$, $M_\infty = 0.3$, $M_t = 0.6$, $B = 8$, $L/\Delta z = N$

Table 4 Propagation speed, V_r/a_∞[a]

ℓ	$N = 40$	$N = 100$
1	0.802	0.800
2	0.809	0.802
3	0.820	0.802
4	0.835	0.806
5	0.854	0.809

[a] $\chi = \pi/2$, $M_\infty = 0.6$, $M_t = 0.7$, $L/\Delta z = N$, V_r/a_∞ (exact) = 0.8

The value of S is influenced by the mesh spacing (Δz,$\Delta\theta$), the order of the Fourier harmonics (ℓ), the flight Mach number (M_∞), and the blade-tip rotational Mach number (M_t). Table 1 gives typical values of S for an eight-blade propfan at cruise condition ($M_\infty = 0.8$, $M_t = 0.8$). It is easy to see that if fewer than 40 points per blade length are used the magnitude of the spurious radiation is not negligible. In general, smaller mesh size helps to reduce this kind of error. In addition, as the Fourier harmonic number increases, the relative magnitude of the spurious radiation increases. Table 2 shows the value of S when the flight Mach number is reduced to 0.3. As can be seen, there is a considerable drop in spurious radiation with a drop in forward flight Mach number. Table 3 gives the values of S as the blade-tip rotational Mach number is reduced to 0.6. This table suggests that there is a further reduction in spurious radiation with a decrease in blade-tip rotational Mach number. In summary, the relative magnitude of spurious radiation increases with mesh size, harmonic number, flight Mach number, and blade-tip rotational Mach number. At transonic Mach number, it could be a significant fraction especially for the higher ($\ell > 3$) harmonics.

Propagation Speed

Formulas (31) and (33) give the acoustic pressure field of the propeller in the blade-fixed coordinate system. The corresponding pressure fields in the stationary frame of reference are found by replacing θ in these formulas by ($\theta_s - \omega t$). It is easy to see from Eq. (31) that the wave fronts form a spiral pattern propagating radially outward with a velocity $V(\chi)$ given by formula (32). This propagation speed is independent of the rotational frequency ω and Fourier harmonic number ℓ. The same speed of propagation V_r for the finite difference solution may be found from Eq. (30):

$$V_r = \omega\ell B/F(k_0) \tag{35}$$

where V_r is, however, a function of the mesh size ($\Delta z/L$,$\Delta\theta$) and the Fourier harmonic number ℓ. Table 4 shows typical values of V_r/a_∞ at $M_\infty = 0.6$, $M_t = 0.7$ for acoustic disturbances propagating in the propeller plane. The exact speed of propagation [from Eq. (32)] is 0.8. It is clear from this table that the propagation speed as calculated by the finite difference solution is higher. Also the speed increases with increase in mesh size. A much larger increase takes place with harmonic number ℓ. At $N = 40$ the propagation speeds of the fourth and fifth harmonics exceed those of the fundamental by nearly 5%.

Amplitudes of the Fourier Components

The amplitudes of the Fourier components of the exact solution can be easily calculated using Eq. (31). The corresponding Fourier amplitudes of the finite difference solution in the

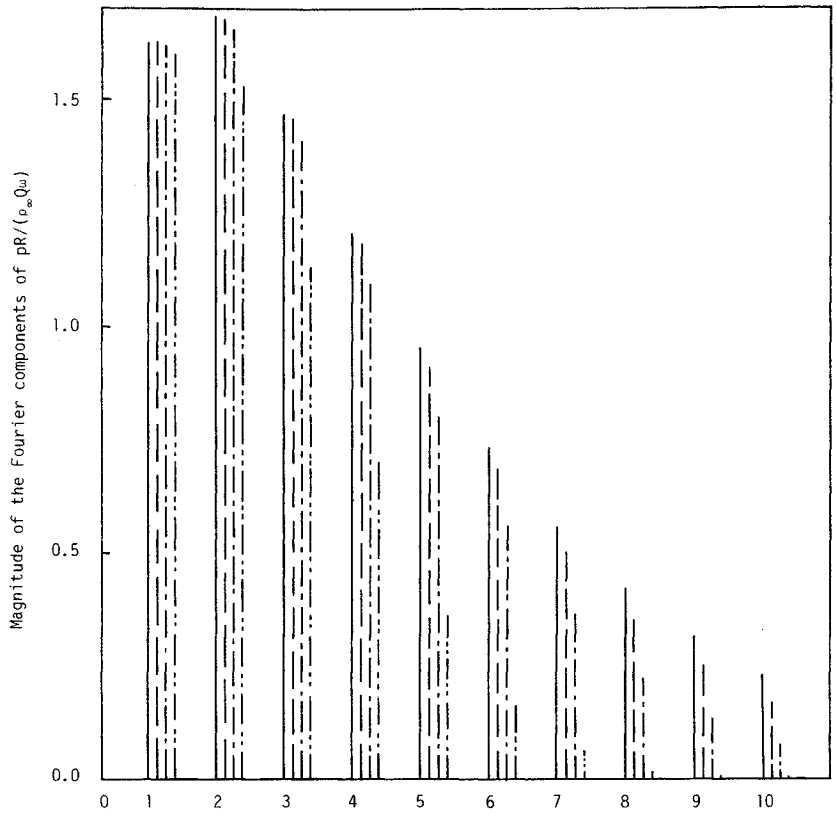

Fig. 2 Magnitudes of different Fourier components, eight blades, $M_\infty = 0.6$, $\omega L/a_\infty = 0.7$; ———, exact solution (PDE); finite difference solution, $L/\Delta z = N$; ———, $N = 200$; —·—·—, $N = 100$; —··—··—, $N = 40$.

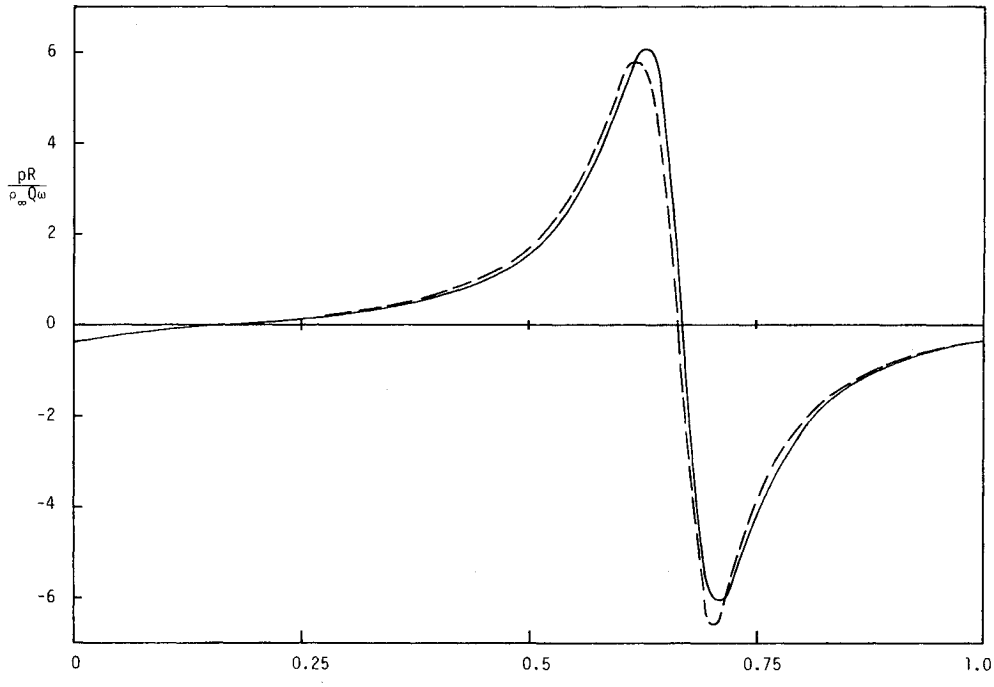

Fig. 3 Pressure waveform over one blade passage period; $M_\infty = 0.6$, $\omega L/a_\infty = 0.7$, $\chi = \pi/2$, $R/L = 3.0$, $B = 8$; ———, exact solution (PDE); -------, finite difference solution, $L/\Delta z = N = 500$.

propeller plane are given by Eq. (33). In the latter case, the amplitudes are functions of the mesh size. Figure 2 shows typical Fourier amplitudes for the first 10 harmonics at $M_\infty = 0.6$ and $M_t = 0.7$ for an eight-blade propeller in the propeller plane. Three mesh sizes are included. As can be seen, the amplitudes of the first two harmonics are well predicted by the finite difference solution using as few as 40 points per blade ($N = 40$). However, for the higher harmonics a larger number of mesh points per blade, e.g., $N = 100$, is needed to give adequate prediction. It is to be noted that within the inviscid fluid model used in the analysis the amplitudes of the Fourier components vary only inversely as the radial distance. This is due to spherical divergence.

Waveform

The pressure waveform over one blade passage period as measured by a microphone in the propeller plane can be cal-

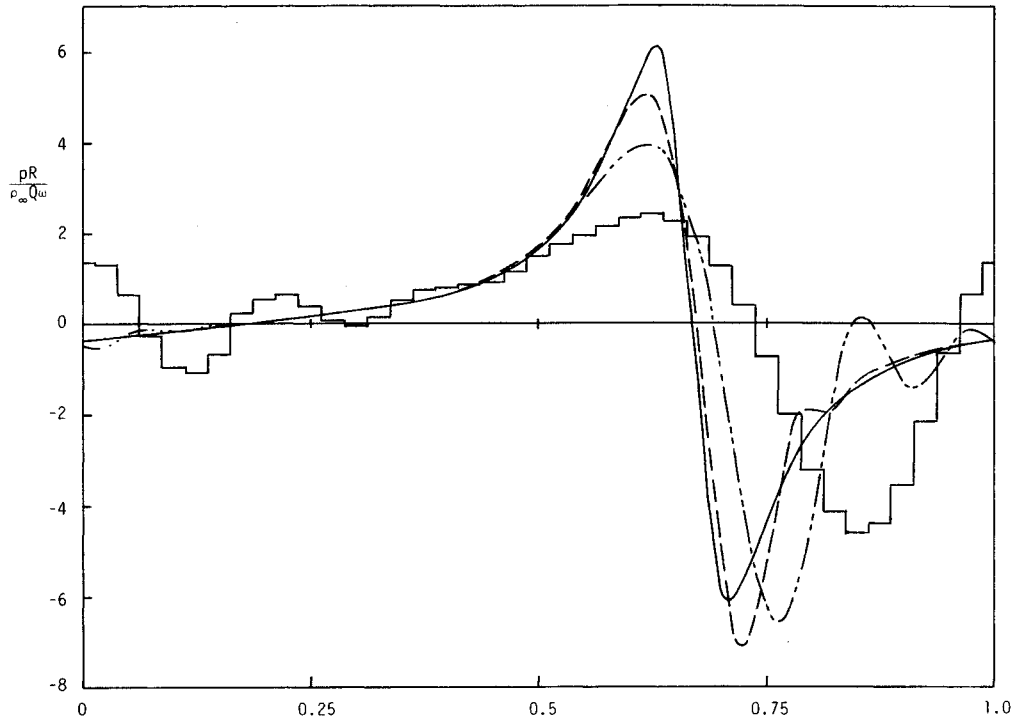

Fig. 4 Pressure waveform over one blade passage period; $M_\infty = 0.6$, $\omega L/a_\infty = 0.7$, $\chi = \pi/2$, $R/L = 3.0$, $B = 8$; ———, exact solution (PDE); finite difference solution, $L/\Delta z = N$; ———, $N = 200$; —·—·—, $N = 100$; ⌐¬⌐¬, $N = 40$.

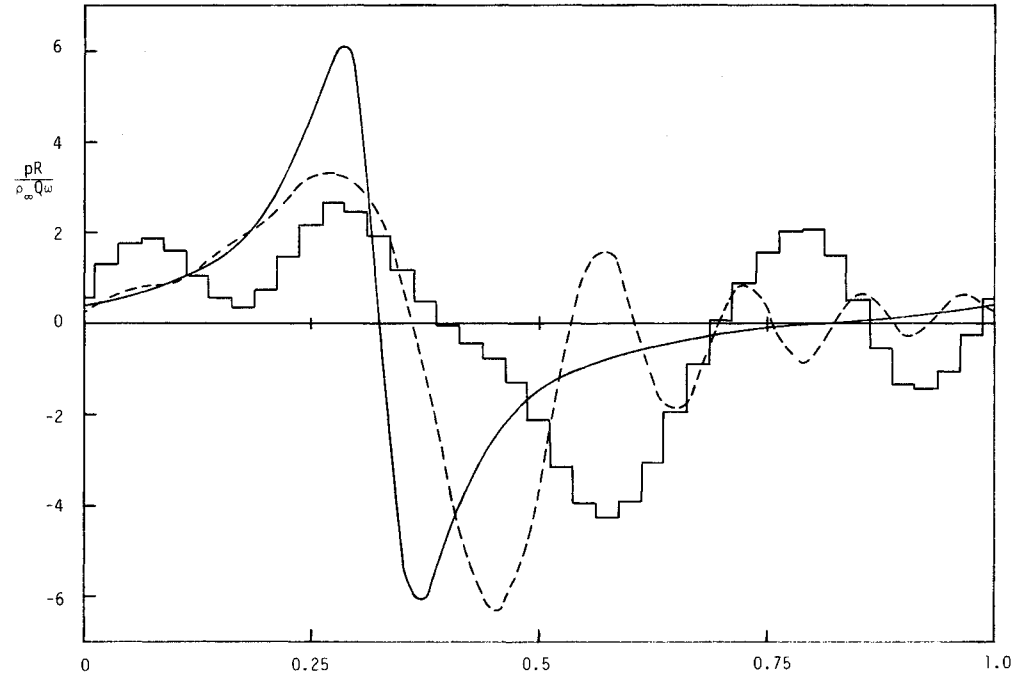

Fig. 5 Pressure waveform over one blade passage period; $M_\infty = 0.6$, $\omega L/a_\infty = 0.7$, $\chi = \pi/2$, $R/L = 6.0$, $B = 8$; ———, exact solution (PDE); finite difference solution, $L/\Delta z = N$; ———, $N = 100$; ⌐¬⌐¬, $N = 40$.

culated by summing over the contributions of the different Fourier components according to Eqs. (31) and (33). A typical case with $M_\infty = 0.6$ and $M_t = 0.7$ for an eight-blade propeller will now be examined. Figure 3 shows the exact waveform [Eq. (31)] and the finite difference solution with 500 mesh points per blade at a radial distance of $R/L = 3.0$. As can be seen, there is excellent agreement between the two waveforms. Figure 4 compares the exact waveform and those of the finite diffference solutions at $R/L = 3.0$ with $N = 200$, 100, and 40. It is evident that as the mesh size increases the waveform deviates more and more from the exact shape. Spurious oscillations at 0.8 of the period begin to show up for N as large as 200. By using 100 points per blade, the calculated waveform contains two well-defined extraneous oscillations. For $N = 40$ the waveform is so swamped with oscillations that it is difficult to say if it resembles the exact solution. Now if the observer is moved farther away from the propeller, say to $R/L = 6.0$, the exact waveform is unchanged. Only the time of arrival of the pressure pulse is shifted. This is shown in Fig. 5. Also shown in this figure are the waveforms for $N = 100$ and 40. At this larger distance these waveforms no longer have a pulse shape. They are dominated by oscillations. It is clear

that unless a very large number of mesh points is used the finite difference approximation fails completely to predict an accurate waveform. Figures 4 and 5 illustrate the effect of dispersion on finite difference solution of propeller noise problems. The pulse shape of the exact waveform is made up of the contributions of different Fourier components precisely phase aligned to cancel out the oscillations of the individual component. Now in the finite difference solution different Fourier components propagate with different velocities. Thus although the amplitudes of the Fourier components are adequately predicted, the relative phase of any two components deviates increasingly as the acoustic wave propagates away from the propeller. This dispersive effect causes a decancellation of the oscillations of the Fourier components so that the waveform becomes more and more oscillatory as the distance of propagation increases. In this sense dispersion error is nonlocal and cumulative in nature.

V. Summary

Finite difference solutions of propeller noise problems are subject to global errors due to dispersion. Dispersive effects greatly distort the calculated pressure waveform as the acoustic disturbances propagate outward. The degree of dispersion depends specifically on the finite difference scheme used. Thus only the least dispersive difference method should be used for computing this class of aeroacoustics problems. In addition, it is found in this paper that spurious radiation is possible when finite difference solutions are constructed. The spurious radiation is a form of aliasing error. It appears that it is of significance only at high subsonic flight Mach number or at high subsonic blade-tip rotational mach number.

Acknowledgment

This work was supported by the Office of Naval Research under Grant N00014-89-J-1836.

References

[1]Farassat, F., "Linear Acoustic Formulas for Calculation of Rotating Blade Noise," *AIAA Journal*, Vol. 19, No. 9, 1981, pp. 1122–1130.

[2]Farassat, F., "Prediction of Advanced Propeller Noise in the Time Domain," *AIAA Journal*, Vol. 24, No. 4, 1986, pp. 578–584.

[3]Hanson, D. B., "Helicoidal Surface Theory for Harmonic Noise of Propellers in the Far Field," *AIAA Journal*, Vol. 18, No. 10, 1980, pp. 1213–1220.

[4]Hanson, D. B., "Influence of Propeller Design Parameters on Far Field Harmonic Noise in Forward Flight," *AIAA Journal*, Vol. 18, No. 11, 1980, pp. 1313–1319.

[5]Hanson, D. B., "Near-Field Frequency-Domain Theory for Propeller Noise," *AIAA Journal*, Vol. 23, No. 4, 1985, pp. 409–504.

[6]Tam, C. K. W., and Salikuddin, M. "Weakly Nonlinear Acoustic and Shock-Wave Theory of the Noise of Advanced High-Speed Turbopropellers," *Journal of Fluid Mechanics*, Vol. 164, 1986, pp. 127–154.

[7]Vichnevetsky, R., and Bowles, J. B., *Fourier Analysis of Numerical Approximations of Hyperbolic Equations*, Society for Industrial and Applied Mathematics, Philadelphia, PA, 1982.

[8]Trefethen, L., "Group Velocity in Finite Difference Schemes," *SIAM Review*, Vol. 24, April 1982, pp. 113–136.

[9]Olver, F. W. J., *Asymptotics and Special Functions*, Academic Press, New York, 1974.